EFFECTS OF THERMAL RELAXATION
ON
AN AMORPHOUS SUPERCONDUCTING
Zr-Rh ALLOY

A. J. Drehman and W. L. Johnson

MASTER

MAY 1978

W. M. KECK LABORATORY OF
ENGINEERING MATERIALS

CALIFORNIA INSTITUTE OF TECHNOLOGY

PASADENA

DISCLAIMER

This report was prepared as an account of work sponsored by an agency of the United States Government. Neither the United States Government nor any agency Thereof, nor any of their employees, makes any warranty, express or implied, or assumes any legal liability or responsibility for the accuracy, completeness, or usefulness of any information, apparatus, product, or process disclosed, or represents that its use would not infringe privately owned rights. Reference herein to any specific commercial product, process, or service by trade name, trademark, manufacturer, or otherwise does not necessarily constitute or imply its endorsement, recommendation, or favoring by the United States Government or any agency thereof. The views and opinions of authors expressed herein do not necessarily state or reflect those of the United States Government or any agency thereof.

DISCLAIMER

Portions of this document may be illegible in electronic image products. Images are produced from the best available original document.

California Institute of Technology.

W. M. Keck Laboratory of Engineering Materials

EFFECTS OF THERMAL RELAXATION

ON AN AMORPHOUS SUPERCONDUCTING Zr-Rh ALLOY

by

A. J. Drehman and W. L. Johnson

MAY 1978

NOTICE

This report was prepared as an account of work sponsored by the United States Government. Neither the United States nor the Department of Energy, nor any of their employees, nor any of their contractors, subcontractors, or their employees, makes any warranty, express or implied, or assumes any legal liability or responsibility for the accuracy, completeness or usefulness of any information, apparatus, product or process disclosed, or represents that its use would not infringe privately-owned rights.

ABSTRACT

The electronic and superconducting properties of an amorphous transition metal alloy are used to evaluate the effects of low temperature annealing. It is observed that the superconducting transition temperature and the electrical resistivity relax exponentially in time from their initial value to a final relaxed value. From this an activation energy for the relaxation process is derived and an explanation is suggested which involves internal stress.

I. INTRODUCTION

It has been shown that amorphous transition metal alloys obtained by rapid quenching from the liquid state exhibit improved magnetic properties [1-4] when annealed at temperatures sufficiently low as to produce no crystallization. Stress relaxation and embrittlement [2], a relaxation of the Curie temperature [5], a change in the atomic pair correlation function [6], and a structural relaxation in the atomic configuration function [7] have also been observed as a result of such annealing. Considering the change in the magnetic properties following such annealing, one might expect effects on the superconducting properties of such materials. Superconductivity is strongly affected by the microscopic structure of the material. Thus one could use such parameters as the transition temperature, the upper critical field, etc. to probe the changes in the microscopic state of the amorphous material following thermal relaxation.

In this investigation the effects of low temperature annealing on the superconducting properties and electrical resistivity of an amorphous alloy have been studied. These properties are then compared to those of the same sample following crystallization. Density measurements as well as x-ray diffraction data were used to complement this study.

The alloy chosen for this study was $Zr_{75}Rh_{25}$ owing to its simplicity (being a binary alloy), the knowledge that it can be prepared in the amorphous state by liquid quenching techniques, and the fact that the alloy is superconducting in the amorphous state [8] as well as in the crystalline state [8-9]. Most amorphous alloys prepared by liquid quenching contain three or more constituents [1-7]. A binary alloy is presumably easier to analyze.

II. EXPERIMENTAL PROCEDURE

A. Sample Preparation

Both the zirconium and the rhodium used in this study were 99.9% pure. Ingots weighing one to four grams were prepared by induction melting on a water cooled silver boat under an argon atmosphere. To assure no oxygen contamination during the preparation of the ingot, a titanium getter was first melted in order to absorb residual oxygen. Thorough mixing of the ingot's constituents was assured by repeated melting and by turning the ingot over between melts. The ingots were subsequently broken and checked for homogeneity.

Amorphous foils were prepared using a liquid quenching technique described in reference [10]. Foils used for study were shown to have less than a few percent crystalline inclusions by volume, as determined by x-ray diffraction data. The foils were cut into small strips for use in the measurements. Typically foils were 30 to 50 μm thick with an area of a few square centimeters and the strips were typically 1 mm by 5 mm in size.

B. Heat Treatment

The samples were sealed in evacuated quartz tubes during heat treatments. The temperature was measured by a mercury thermometer for temperatures below 300°C. A thermocouple was used for higher temperatures involved in investigating part of the equilibrium crystalline phase field. The furnace temperature was stable to ± 2 C during typical times used for heat treatments.

C.   X-ray Diffraction

The structure of the ingots and the liquid quenched foils was deter-
mined from the x-ray diffraction data obtained using a standard x-ray
diffractometer (Ni filtered Cu Kα radiation). Amorphous foils were
rejected if they initially contained any detectable crystalline phase
inclusions as determined from the diffraction data. This criterion
assures that the amount of crystalline inclusions is less than a few
percent of the sample by volume.

A more accurate scan was obtained using a step scanning diffracto-
meter (Mo Kα radiation). This data was used to determine the detailed
characteristics of the x-ray pattern.

D.   Density Measurements

The density of ingots and foils was measured by the method of hydro-
statics weighing (Archimedes' method) using toluene as the working fluid
as described in reference [11]. Care had to be taken to make sure that
the sample was free of any deposits (finger oil, etc.) and that no air
bubbles adhered to the foils when they were submerged into the toluene
bath. Each sample was cleaned before weighing and irregular edges were
removed. Measurements had an RMS standard deviation of 0.07% for ingots
and 0.1% for liquid quenched foils.

E.   Superconducting Transition Temperature (T_c)

The induction method was used to measure T_c. Samples were placed in
a small copper coil which forms one arm of an AC inductance bridge. The
change in inductance due to the Meissner effect was measured as a

function of temperature through the use of a calibrated Germanium resistance thermometer. The criterion for T_c was taken to be the temperature at which half of the total change in the inductance is observed. Typically the width of the transition is several hundredths of a degree (K). The entire assembly (samples, coils, thermometer, etc.) are located in a copper exchange gas cylinder. The temperature can be varied using a heating element also located in the exchange gas cylinder.

F. Resistivity Measurements

The resistivity of a small strip of amorphous $Zr_{75}Rh_{25}$ was measured as a function of time during annealing at a constant temperature. The sample was kept under a helium atmosphere and in close proximity to a titanium getter in order to prevent oxidation during the annealing period. A four point probe technique was used with the voltage and current lead spot welded to the strip. The absolute resistivity had previously been measured for unrelaxed foils, so only the change in resistivity was measured. The annealing temperature was measured by a Pt-PtRh thermocouple.

G. Upper Critical Field Measurements (H_{c2})

The upper critical field was determined by measuring the sample resistance as a function of the applied magnetic field at a series of different temperatures. The resistance was measured using a standard four point probe technique. The current density was approximately 0.5 amps/cm^2 (corresponding to a 0.1 milliamp current source). The temperature was determined by measuring the vapor pressure above the helium bath in which the sample was submerged. Magnetic fields ranging up to 40 kG were supplied by a niobium-titanium superconducting solenoid.

The upper critical field is defined as the maximum field for which superconductivity exists in the bulk specimen at a fixed temperature. When the sample resistance is measured as a function of applied field, a well-defined rise in resistance occurs over a narrow field interval. For definitiveness, H_{c2} was defined as the field for which the sample resistance is 50% of the normal state value. By using an x-y plotter, resistance versus applied magnetic field was traced for a number of fixed temperatures.

III.   RESULTS

A.   Thermal Relaxation of the Amorphous State

Amorphous foils were obtained near the composition of 75% Zr, 25% Rh as reported in reference [8]. This composition falls near a deep eutectic, as is common in liquid quenched amorphous materials. Although all of the properties measured (superconducting transition temperature, the upper critical field as a function of temperature, density, electrical resistivity, and the x-ray diffraction pattern) varied slightly from foil to foil, the effects of annealing on the properties were substantially the same.

The effect of annealing on T_c is illustrated in Fig. 1 where the relative inductance vs. temperature is shown for two strips of the same foil, one "as quenched", the other partially relaxed. The superconducting transition temperature (T_c) of the "as quenched" (unrelaxed) amorphous foils varied by roughly 0.08 K over the range 4.30 to 4.38 K. The decrease in T_c, as a result of full annealing, was between 0.20 and 0.30 K. Therefore a series of strips from a single foil were used in order to obtain a relaxation curve at a particular annealing temperature. This
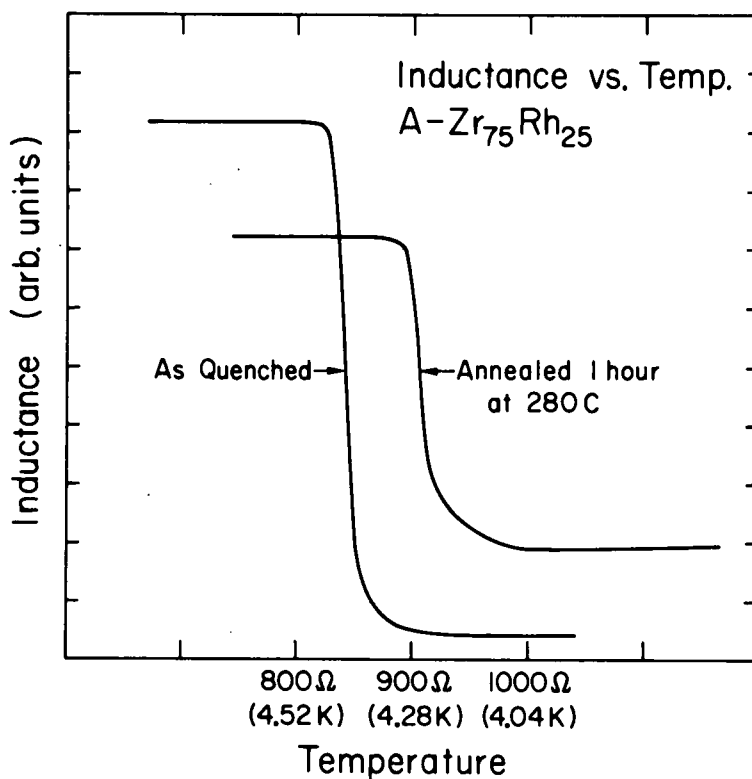
Fig. 1. Relative inductance as a function of temperature for partially relaxed and unrelaxed amorphous $Zr_{75}Rh_{25}$.

procedure was repeated at different annealing temperatures using several different foils in order to get a representative sampling of foils. The relaxation curves were plotted with $\Delta T_c(t)/\Delta T_c(\infty)$ vs. annealing time (t). $\Delta T_c(\infty)$ is the total shift in T_c of the foil used, and $\Delta T_c(t)$ is the shift in T_c after time t. The results are shown in Fig. 2. Table I lists $T_c(0)$ and $\Delta T_c(\infty)$ for the foils used.

The upper critical field (H_{c2}) was measured for a partially relaxed and an unrelaxed strip from a single foil. In Fig. 3, the resistance vs. applied field are plotted for various temperatures. From this an $H_{c2}(T)$ vs. temperature (T) plot can be made for each sample. Over the temperature range measured (3.0 to 4.2 K), H_{c2} was found to be linear:

$$H_{c2}(T) = (dH_{c2}/dT)_{T_c} (T-T_c) \qquad (T \leq T_c)$$

where

$$-dH_{c2}/dT = 30 \pm 1 \text{ kG/K}$$

for both samples. The partially relaxed sample had an H_{c2} approximately 4.2 kG lower than the unrelaxed sample due to the lower T_c of the partially relaxed sample. This corresponds to a shift in T_c of 0.14 K. Extrapolating from the H_{c2} data one gets a T_c of 4.38 ± 0.01 K for the unrelaxed sample. From the inductance measurements of T_c, it was found that the T_c of the unrelaxed sample was 4.38 K. For the partially relaxed sample $\Delta T_c(t)/\Delta T_c(\infty) = 0.72$ and $\Delta T_c(\infty) = 0.21$ K. This gives a shift in T_c of 0.15 K. This serves as a consistancy check between the inductively measured T_c, and the H_{c2} measurements.
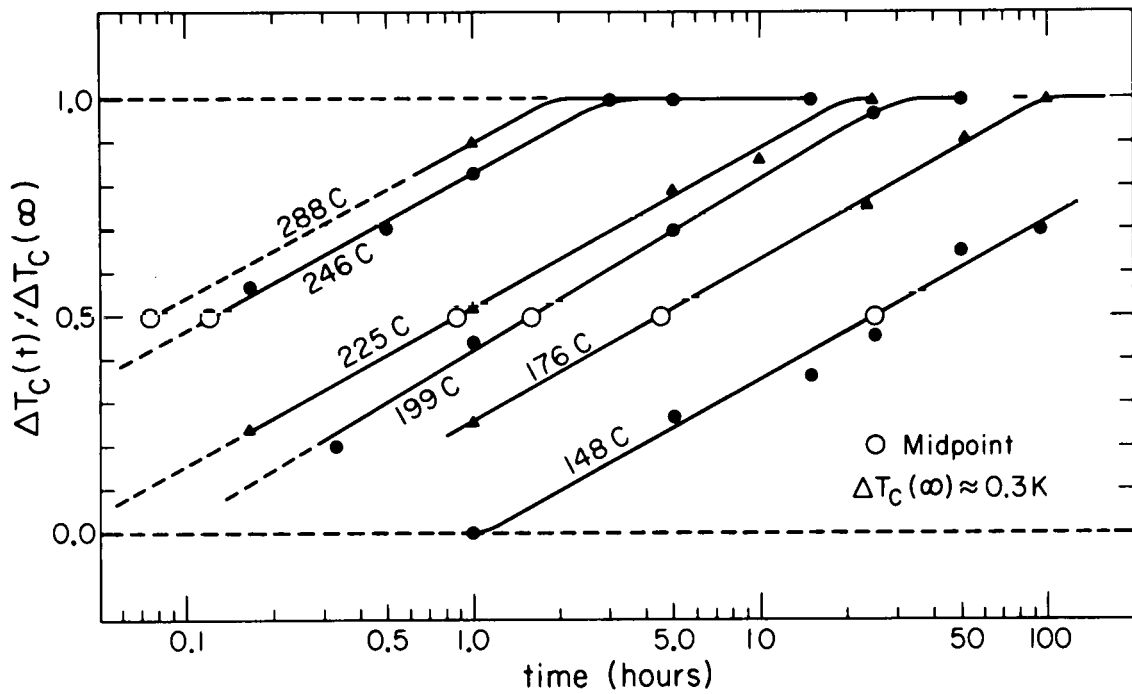
Fig. 2.   Relaxation of the superconducting transition as a function of time at various annealing temperatures.

TABLE I.   List of the superconducting transition temperatures for the
samples used and the temperature at which they were later
annealed.

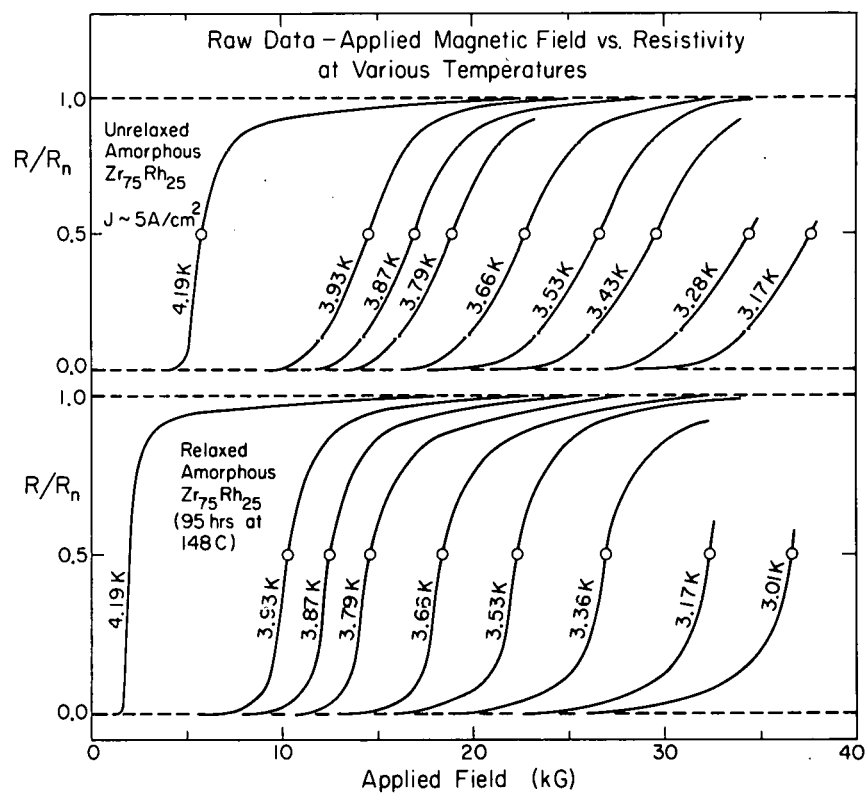| T_c	$\Delta T_c(\infty)$	annealing temperature
4.32	.20	280 and 288 C
4.38	.30	246 and 225 C
4.30	.21	199 and 148 C
4.33	.28	176 and 269 C

Fig. 3. Resistance as a function of field; used to determine the upper critical field as a function of temperature.

Density measurements were made on a foil section (having an area of approximately 3 cm^2) both before and after annealing at 288 C. The density before annealing was 7.570 ± .005 gm/cc and after annealing at 246 C for 3 hours it was 7.581 ± 0.007 gm/cc. This gives a change in density of 0.15 % ± 0.11%. Unfortunately, the error in the density difference is of the order of the difference itself. The density of several other unrelaxed foils were measured and fell within the range of 7.57 ± 0.01 gm/cm^3.

The resistivity of the unrelaxed amorphous state has been reported to be approximately 220 ± 30 μΩcm at room temperature [12]. As with some other amorphous metals, the temperature coefficient of resistivity is negative over the range of 4.2 K to 300 C, and is approximately:

$$(1/\rho) \, d\rho/dT = - 9.4 \times 10^{-5} \pm 1 \times 10^{-6}/K$$

over the range 100 C to 300 C. By measuring the resistance of a strip during annealing at 269 C, a 4.4% ± 0.2% decrease in the resistivity was observed between the unrelaxed and fully relaxed states. Fig. 4 gives this relaxation curve. Taking the midpoint of the resistivity relaxation curve and comparing it to the T_c relaxation curves, one finds that the two are in good agreement. Also it is interesting to note that the change in resistivity due to annealing (4.4%) is of the same order as its change in T_c (6.5%). (See Table I.)

In addition to using x-ray diffraction data to determine whether there are crystalline inclusions present in the amorphous foils, a detailed step scanning x-ray pattern was made of an unrelaxed sample and the same fully relaxed. The scan was made using Mo Kα radiation, and the sample consisted of a mosaic of several foils in order to obtain a large surface area for
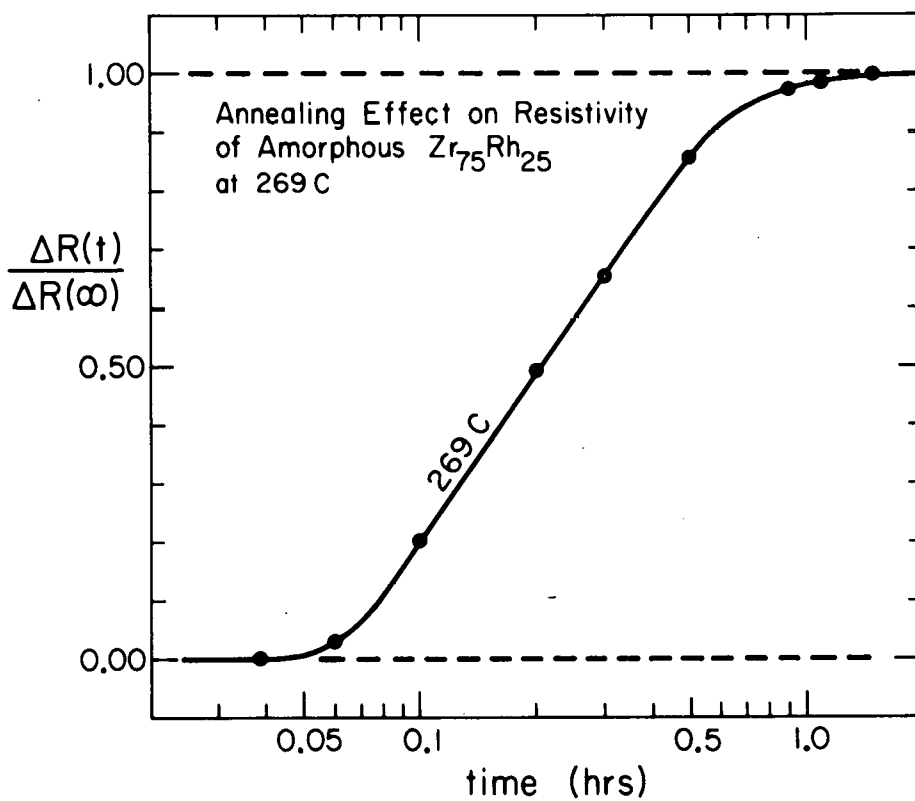
Fig. 4.   Electrical resistivity as a function of time for an annealing

temperature of 269 C.

scattering. The total counts per scan step are listed on either side of the diffraction patterns in Fig. 5. The left side corresponds to the unrelaxed state, and the right side to the relaxed state. The relaxed sample was annealed for 3.5 hours at 255 C. The peak of the first amorphous band occurs at 16.57 ± 0.01° for the relaxed state, and at 16.49° ± 0.01° for the unrelaxed state. Using the standard formula for the nearest neighbor distance [3]:

$$d_{eff} \cong (3/2)^{\frac{1}{2}} (\lambda/2\sin\theta)$$

where

$$\lambda = .710688 \text{ Å for Mo K}\alpha \text{ radiation.}$$

This gives an effective nearest neighbor distance of 3.020 ± 0.001 Å for the relaxed state, and 3.035 ± 0.001 Å for the unrelaxed state. This corresponds to a small decrease of 0.50% ± 0.04% in the average nearest neighbor distance as given by this formula. This result will be discussed later.

These results demonstrate that the relaxed state and the unrelaxed state have somewhat different electrical and structural properties. Another property which was not quantitatively studied was stress relaxation. Foils subjected to a stress during annealing relax mechanically. This was observed when a foil placed in a quartz tube for annealing was bent to fit the curvature of the tube. Upon removal after annealing it was observed that the foil partially retained the curvature of the tube. This does not occur at room temperature. It was also observed that if one surface of the foil was lightly sandpapered, then the foil became concave, bending away from the sandpapered surface. This indicates the presence of internal stresses in the "as quenched" foil.
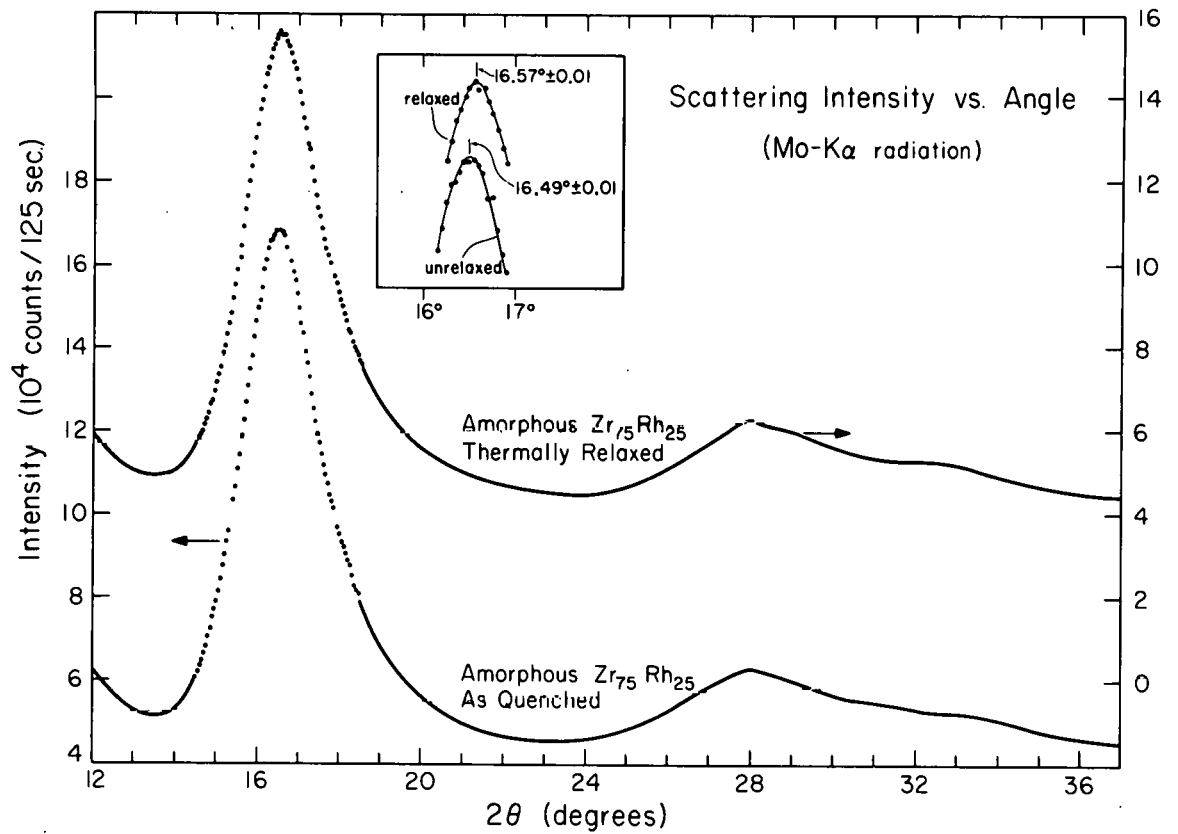
Fig. 5.   X-ray diffraction scan for the same sample before and after annealing at 255 C for 3.5 hours.

B. High Temperature Heat Treatment and Crystallization

High temperature heat treatment of amorphous $Zr_{75}Rh_{25}$ (relaxed or unrelaxed) resulted in crystallization. Heat treatment at 360 C for 5 hours resulted in a metastable single phase having an $E9_3$ structure [9] (space group Fd 3m). This structure was verified by x-ray diffraction data. The T_c of the $E9_3$ structure was determined to be between 2.8 and 2.9 K. This result is in contrast with the previously reported value of 11.0 K [9]. (In the present study, only samples containing the C-16 phase Zr_2Rh were observed to have a T_c near 11 K.) Further heat treatment at 600 C for one hour returns the alloy to its equilibrium structure of αZr + Zr_2Rh. The αZr phase has an hcp structure with a solubility for Rh of less than 0.1% [15]. The x-ray pattern of the Zr_2Rh phase was indexed as a C-16 structure. A model of the C-16 structure appears in reference [16]. The T_c of the C-16 structure is approximately 11.2 K as measured inductively. The use of this technique makes it impossible to find the T_c of the αZr solid solution when comparable amounts of the C-16 phase are present. The T_c of αZr has been reported to be much lower than that found for the C-16 structure [9].

The temperature gradient of the upper critical field ($-dH_{c2}/dT$) near T_c was measured to be 30 ± 2 kG/K for the $E9_3$ structure of Zr_3Rh. Reference [14] reports the temperature gradient to be 10.5 kG/K for the equilibrium crystalline phase of Zr_2Rh, which is tentatively identified as a C-16 structure in this study.

Fig. 6 shows a partial phase diagram for the Zr-Rh system. The diagram is based on the previous diagram given in reference [4] and data from this study. The eutectic appears to be located somewhere near the composition of 25% Rh. The $E9_3$ phase does not appear on the phase diagram
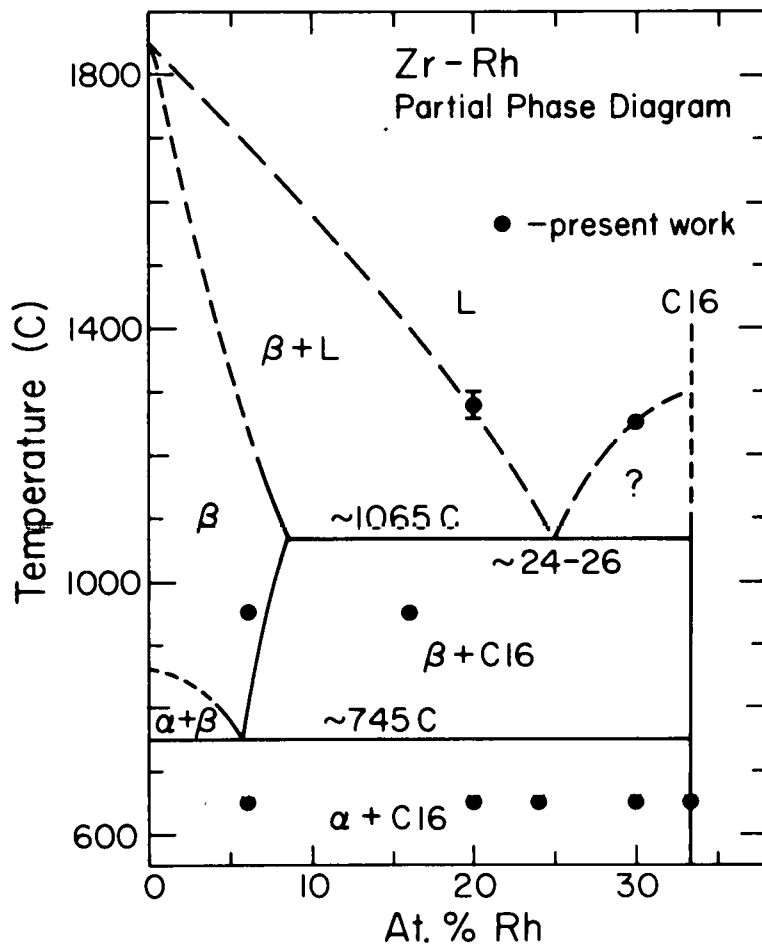
Fig. 6.   The Zr-rich portion of the Zr-Rh phase diagram.

and according to the present study is a metastable phase.

Density measurements were made on a series of ingots (heat treated at 600 C) with varying concentrations of rhodium. From this data a density versus composition graph was made, and is shown in Fig. 7. The density is linear in the concentration of rhodium between 0% Rh and 33 1/3% Rh. This suggests that there are only two phases present, as indicated in the phase diagram. Fig. 7 also includes data for amorphous $Zr_{75}Rh_{25}$ and shows that it is 0.6% ± 0.1% less dense than the corresponding crystalline alloy. The density of the $E9_3$ structure of Zr_3Rh varied somewhat from sample to sample, and fell within the same range of densities as the amorphous state, 7.57 ± 0.01 gm/cm^3.

A summary of the crystalline state properties and the corresponding amorphous state properties appears in Table II. The properties listed are the superconducting transition temperature, the temperature gradient of the upper critical field, density and the heat treatment required to reach that state starting from the unrelaxed amorphous state.

IV. DISCUSSION

Based on the T_c relaxation curves, it is possible to derive an activation energy for relaxation if one assumes that there is a single mechanism by which this relaxation occurs. This assumption is justified by use of the Arrhenius plot shown in Fig. 8. To find the characteristic energy, let $\tau_{\frac{1}{2}}$ be the annealing time required to reach the midpoint on the T_c relaxation curve at a given annealing temperature

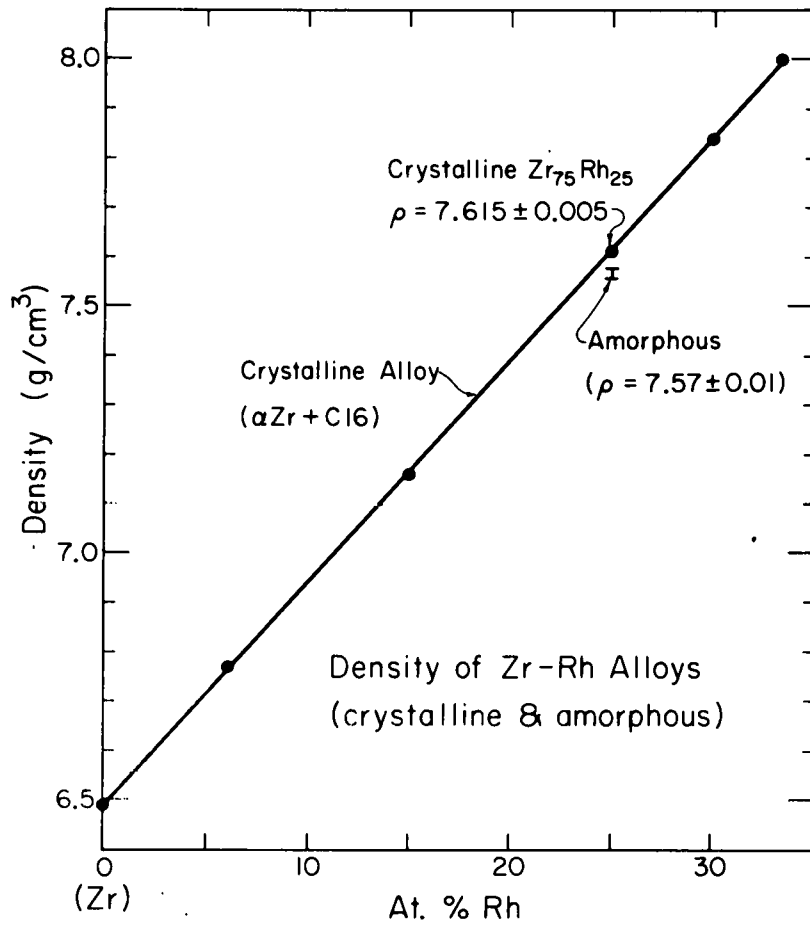$$\Delta T_c \ (\tau_{\frac{1}{2}}) = \frac{1}{2} \Delta T_c(\infty)$$

Fig. 7. Density vs. composition for both the equilibrium crystalline state and amorphous $Zr_{75}Rh_{25}$.

TABLE II.   Characteristic properties of various states of $Zr_{75}Rh_{25}$.

$Zr_{75}Rh_{25}$	Unrelaxed Amorphous	Relaxed Amorphous	Crystalline $E9_3$	Crystalline $\alpha Zr + Zr_2Rh$
Comments	-----	-----	metastable	equilibrium
Heat Treatment*	-----	250 C, 5 hrs.	360 C, 5 hrs.	600 C, 1 hr.
T_c(K)	4.33 ± 0.03	4.08 ± 0.03	2.8 to 2.9	11.20 ± 0.03[†]
$-dH_{c2}/dT$ (kG/K)	30 ± 1	30 ± 1	30 ± 2	$\sim$ 10.5 [14]
density (gm/cm^3)	7.57 ± 0.01	7.58 ± 0.01	7.57 ± 0.01	7.615 ± .005

*   Typical heat treatment required to reach this state from the unrelaxed amorphous state.

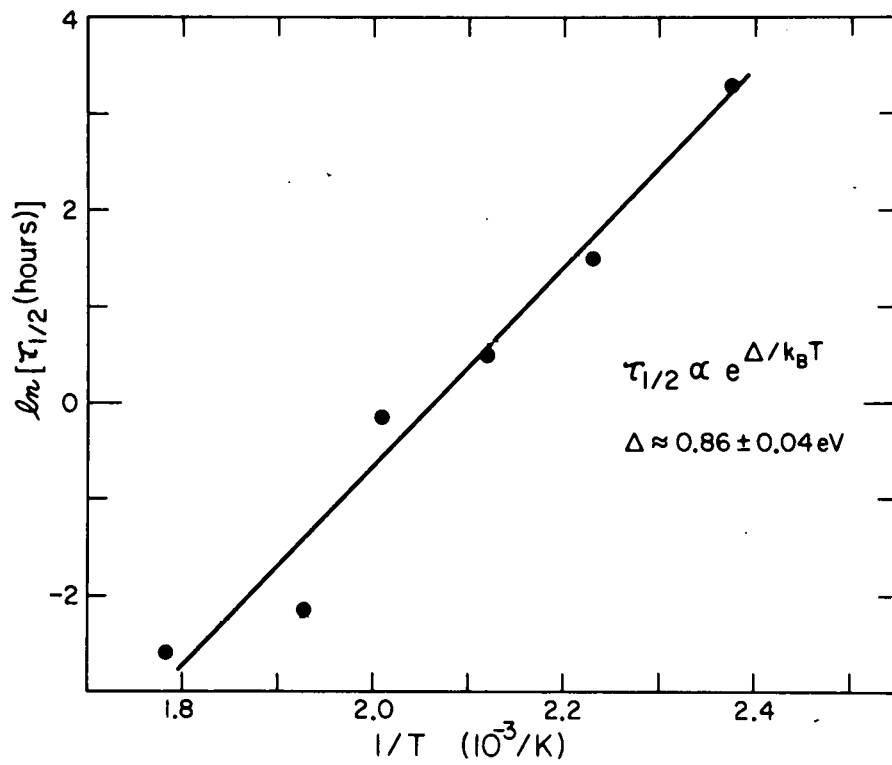†   This applied to the range 15% to 33% Rh for which the Zr_2Rh (C-16) phase is present.

Fig. 8. Arrhenius plot for determining the characteristic activation energy of the relaxation process.

Using the assumption of a single activation energy it follows that:

$$\tau_{\frac{1}{2}} = \tau_0 \exp{(\Delta/k_B T)}$$

where Δ is the activation energy and k_B is Boltzman's constant. Fig. 8 shows the log of $\tau_{\frac{1}{2}}$ in hours versus the inverse of the annealing temperature (T) as given in the relaxation curves of Fig. 2. A single activation energy should result in a straight line with the slope giving the activation energy:

$$\Delta = k_B \, (T_1 T_2)/(T_2 - T_1) \ln{(\tau_1/\tau_2)}$$

where the subscripts on the T's and τ's refer to any two points on the line in Fig. 8, and the subscript $\frac{1}{2}$ on the τ's has been dropped. From this one arrives at an activation energy of:

$$\Delta = 0.86 \pm 0.04 \text{ eV.}$$

Using this activation energy, one can estimate how often a jump over the barrier is attempted. If

$$dN/dt = -N \, \nu \exp{(-\Delta/k_B T)}$$

then

$$\nu = \ln{2} \, (\tau_{\frac{1}{2}})^{-1} \exp{(\Delta/k_B T)}$$

and

$$\nu \simeq 3.4 \times 10^5 \text{ sec}^{-1}.$$

A typical Debye frequency is of the order 10^{13} to 10^{14} sec^{-1}. From this it would seem that the motion of several atoms must somehow coordinate in order for the jump to be possible.

Using x-ray data and the Scherrer formula for calculating nearest neighbor distances, one arrives at a 0.5% decrease in the average nearest neighbor distance. In a very simple picture, this would suggest a densification upon annealing, although it is very difficult to correlate the x-ray results with density change. The fact that the measured density does not change by more than 0.2% leads one to believe that the relaxation process is characterized by rather subtle atomic rearrangements. It was not possible to do a complete radial distribution function calculation during this study, therefore no further comments regarding the details of this rearrangement are possible.

The purpose of determining $H_{c2}(T)$ was twofold. From a measurement of $-dH_{c2}/dT$ one can derive the diffusivity of the material; $D = 1/3 \, V_F \ell$, where V_F is the Fermi velocity and ℓ is the electron mean free path. The fact that the observed $-dH_{c2}/dT$ is the same before and after annealing, can be interpreted to mean that the product of V_F and ℓ is not changed by annealing. A second property of the resistance versus applied field curve at constant temperature is the width of the normal to superconducting transition. In general a sharper transition indicates greater homogeneity of the material. Using the slope of the resistance versus applied field curve (T fixed) taken at the 50% point of the transition curves in Fig. 3, indicates that the transition width of the unrelaxed state is approximately 2.5 times that of the relaxed state over the range 0 to 40 kG. This implies a greater degree of homogeneity in the relaxed state. This result is consistent with a picture in which the unrelaxed specimen contains a macroscopic distribution of internal stresses which are relieved during relaxation. The curvature at the bottom of the resistance versus applied field plot is caused by flux flow in the sample, and the rounding of the

upper part of the curve is associated with fluctuations and surface effects.

In looking at the effects on T_c and resistivity one notes that they both change by about the same amount and both are decreased. These two quantities are not simply connected to one another. The T_c is determined by the electronic band structure which is dominated by the 4d electrons, while the resistivity is primarily determined by the transport properties of the 5s electrons. An analysis of these observations is beyond the scope of this study, but it is hoped that further investigations will be made in this area as it seems to be of use in understanding the properties of the amorphous state.

An explanation of the annealing effects on the electrical properties might involve a relaxation of internal stresses and a change in the distribution of free volume. It has been suggested that internal stresses are frozen into the material during rapid quenching [4,6,17]. These internal stresses could be associated with an inhomogeneous distribution of free volume within the material on a macroscopic scale. Annealing causes homogenization of this free volume and may decrease the total free volume. This explanation is consistent with the resistivity and density measurements, as well as the width of the $H_{c2}(T)$ transition. Stresses tend to increase structural scattering and this would account for a larger resistivity in the unrelaxed state. A decrease in the total free volume would lead to a slight densification of the material. Homogenization upon annealing is indicated by the sharper resistance versus applied field transition of the relaxed state than that of the unrelaxed state. An explanation of the effects on T_c and $-dH_{c2}/dT$ is more difficult as one would need greater knowledge of the microscopic atomic configurations and their theoretical connection with the microscopic parameters which appear in the theory of superconductivity.

V.   CONCLUSION

Low temperature annealing of amorphous $Zr_{75}Rh_{25}$ prepared by rapid quenching from the liquid state results in a change in the superconducting transition temperature, electrical resistance, and homogeneity of the material. The change in these properties is suggested to be the result of a relaxation of internal stresses present in "as quenched" specimens. These stresses are suggested to be associated with an inhomogeneous distribution of free volume in the "as quenched" material. An activation energy for the relaxation processes is found to be approximately 0.86 eV, if one assumes a single relaxation process.

It is hoped that further work on this and other alloys may be used to give a greater insight into the microscopic state of an amorphous material.

REFERENCES

[1.]   T. Egami, P. J. Flanders, C. D. Graham, Jr., Appl. Phys. Letters
        26, 128 (1975).

[2]   H. S. Chen, S. D. Ferris, E. M. Gyorgy, H. J. Leamy, R. C. Sherwood,
        Appl. Phys. Letters, 26, 405 (1975).

[3]   H. Fujimori, T. Masumoto, Y. Obi, M.Kikuchi, Japan. J. Appl. Phys.,
        13, 1889 (1974).

[4]   R. S. Williams, T. Egami, IEEE Trans. Mag., MAG-12, 927 (1976).

[5]   H. S. Chen, R. C. Sherwood, H. J. Leamy, E. M. Gyorgy, IEEE Trans.
        Mag. MAG-12, 933 (1976).

[6]   T. Egami, P. J. Flanders, AIP Conf. Proc., 29, 220 (1976).

[7]   H. S. Chen, E. Coleman, Appl. Phys. Letters, Vol. 28, 245 (1976).

[8]   K. Togano, K. Tachikawa, J. of Appl. Phys., Vol. 46, 3609 (1975).

[9]   Ch. J. Raub, C. A. Andersen, Z. Phys., 175, 105 (1963).

[10]   P. Duwez, Progress in Solid State Chemistry (Pergamon, Oxford, 1966),
        Vol. 3.

[11]   H. Berman, Amer. Mineralogist, 24, 434 (1939).

[12] W. L. Johnson, C. C. Tsuei, P. Chaudhari, Phys. Rev. B, Vol. 17, $\underline{7}$, 2884 (1978).

[13] A. Guinier, X-Ray Diffraction (Freeman, San Francisco, 1963) p. 72.

[14] K. Togono, K. Tachikawa, Rapidly Quenched Metals-Second International Conference Section I, Edited by N. J. Grant, B. C. Giessen (Massachusetts Institute of Technology, 1976) p. 519.

[15] S. T. Zegler, J. Phys. Chem. Solids, $\underline{26}$, 1347 (1965).

[16] F. S. Galasso, Structure and Properties of Inorganic Solids, (Pergamon, Oxford, 1970) p. 254.

[17] F. E. Luborsky, J. J. Becker, R. O. McCary, IEEE Trans. Mag. MAG-11, 1644 (1974).